Analysis of photonic band gaps in two-dimensional photonic crystals with rods covered by a thin interfacial layer

T. Trifonov,[1] L. F. Marsal,[1,*] A. Rodríguez,[2] J. Pallarès,[1] and R. Alcubilla[2]
[1]*Departament d'Enginyeria Electrònica, Elèctrica i Automàtica, ETSE, Universitat Rovira i Virgili, Avda. Països Catalans 26, 43007 Tarragona, Spain*
[2]*Departament d'Enginyeria Electrònica, Universitat Politècnica de Catalunya, Edifici C4, Campus Nord, c/ Jordi Girona 1-3, 08034 Barcelona, Spain*
(Received 2 July 2004; published 15 November 2004)

We investigate different aspects of the absolute photonic band gap (PBG) formation in two-dimensional photonic structures consisting of rods covered with a thin dielectric film. Specifically, triangular and honeycomb lattices in both complementary arrangements, i.e., air rods drilled in silicon matrix and silicon rods in air, are studied. We consider that the rods are formed of a dielectric core (silicon or air) surrounded by a cladding layer of silicon dioxide (SiO_2), silicon nitride (Si_3N_4), or germanium (Ge). Such photonic lattices present absolute photonic band gaps, and we study the evolution of these gaps as functions of the cladding material and thickness. Our results show that in the case of air rods in dielectric media the existence of dielectric cladding reduces the absolute gap width and may cause complete closure of the gap if thick layers are considered. For the case of dielectric rods in air, however, the existence of a cladding layer can be advantageous and larger absolute PBG's can be achieved.

DOI: 10.1103/PhysRevB.70.195108 PACS number(s): 78.20.Bh, 42.70.Qs, 41.90.+e

I. INTRODUCTION

Photonic crystals (PC's) provide an effective way to control and manipulate electromagnetic radiation. They can affect the properties of photons in much the same way as a semiconductor affects the properties of electrons.[1] One of the main features of PC's is that they can be designed to exhibit an absolute photonic band gap: a frequency region where electromagnetic waves are prohibited to propagate in the crystal, regardless of the polarization or propagating direction. This may bring about some unusual physical phenomena, such as light localization[2] and inhibited spontaneous emission.[3] Applications of PC's in semiconductor lasers,[4] optical fibers,[5] single-mode waveguides,[6] etc. have been proposed. However, three-dimensional (3D) photonic crystals are still very difficult to fabricate at optical length scales. Two-dimensional PC's are easier to fabricate than 3D ones, especially for the technologically important near-IR spectrum. Much attention has therefore been paid to 2D PC's which have been mainly investigated for triangular,[7] square,[8] and hexagonal[9] lattices with various cross sections of the dielectric scatterers.[10–12]

Unlike the numerous studies of 2D PC's with diverse arrangements and scatterers, to our knowledge few authors have studied how the existence of an interfacial (or cladding) layer affects the properties of photonic gaps in 2D crystals. This interfacial layer could be the unwanted result of the fabrication process itself. For example, a promising technique for the fabrication of 2D PC's for the near-IR spectrum is the electrochemical etching of silicon in acid solutions.[13] Macroporous silicon formed by this technique exhibits uniform pores with a diameter of less than 1 μm and an aspect ratio (the ratio of pore length to pore diameter) of several hundreds of micrometers. After etching, the macropores are covered by a thin microporous layer[14] that can be treated as an interfacial layer between the pores (air rods) and background medium. The effective refractive index of this interfacial layer is less than the refractive index of silicon and depends on the sample characteristics and etching conditions. The existence of such an interfacial layer will influence the properties of photonic gaps in 2D photonic crystal. Very recently, Pan and Li[15] have studied the effects of the etching interfacial layers on the absolute photonic band gap (PBG) in 2D triangular structure. However, they did not consider the inverse structure—namely, dielectric rods in air. It is well known that the honeycomb lattice formed of dielectric rods in air does exhibit absolute PBG's. These absolute PBG's arise for filling fractions far from the close-packed condition and therefore greatly favor the fabrication of 2D photonic crystals. In addition, when the aim is the fabrication of semiconductor active devices, the use of dielectric rods in air instead of holes in dielectric media is advantageous.[16] An important loss mechanism in these active devices is the nonradiative surface recombination at the sidewalls of the active media. A common strategy for reducing the surface recombination is passivating the semiconductor surfaces by a thin dielectric film. Therefore the interfacial layer in this case is a requirement and it should be intentionally formed.

In this context, we think that it is also important to study how the existence of some dielectric cladding affects the PBG formation in 2D photonic crystals of both complementary arrangements: air rods in dielectric media and dielectric rods in air. The aim of the present work is therefore to analyze the absolute PBG formation for triangular and honeycomb photonic structures consisting either of air rods (holes) in silicon or silicon rods in air. The rod surface, in the case of silicon rods, and hole walls, in the case of air rods, are covered with an interfacial layer of varied thickness. The rod and the surrounding interfacial layer can be treated as a single rod having a core and cladding regions. We considered three different materials for the dielectric cladding: silicon dioxide (SiO_2), silicon nitride (Si_3N_4), or germanium (Ge).

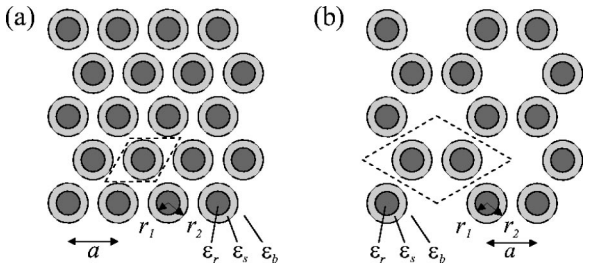

FIG. 1. Schematic representation of the studied structures: (a) triangular lattice of circular rods, (b) honeycomb lattice of circular rods. The rods are covered by a shell layer with dielectric constant ε_s different from the dielectric constant of the rods ε_r and that of the background media ε_b. The lattice unit cell is indicated by a dashed line.

They have been chosen for the following reasons. The SiO_2 and Si_3N_4 are commonly used as passivating materials in the silicon industry. A fully established technique for growing SiO_2 or Si_3N_4 layers exists, that permits fine control of the layer thickness. Besides, the refractive indexes of SiO_2 and Si_3N_4 are less than that of silicon and they cover in part the refractive-index range of microporous silicon mentioned above. Thereby, the results considering etched pores "covered" with the SiO_2 or Si_3N_4 layer will be also valid for the case of pores walls covered with microporous silicon. Germanium has been mainly chosen because it has a refractive index greater than that of silicon. Thus we are not restricted to study only lower-refractive-index materials because deposition of the Ge interfacial layer is also possible, for instance by plasma-enhanced chemical vapor deposition technique.

II. LATTICE DESCRIPTION AND NUMERICAL METHOD

The structures under consideration are depicted in Fig. 1, where (a) is a triangular lattice of inner rods and outer interfacial (shell) layer and (b) is the honeycomb lattice of inner rods and outer shell layer. Parameters ε_r, ε_s, and ε_b denote the dielectric constants of the inner rod, shell layer, and background medium, respectively. When air holes in silicon are considered the dielectric constants of the inner rods and background medium are fixed to be $\varepsilon_r=1$ and $\varepsilon_b=12.096$ (silicon at wavelength $\lambda=1.55$ μm).[17] For silicon rods in air, the values of the parameters are reversed: $\varepsilon_r=12.096$ and $\varepsilon_b=1$. The shell-layer dielectric constant ε_s for the three different materials considered here is: (i) $\varepsilon_s=3.9$ for SiO_2, (ii) $\varepsilon_s=7.5$ for Si_3N_4, and (iii) $\varepsilon_s=16$ for Ge.[17] The dielectric constant of the shell layer is therefore fixed to be less than the dielectric constant of silicon for the first two cases and greater than the dielectric constant of silicon for the third case. Parameter a is the distance between the centers of two nearest-neighbor rods. For the triangular structure, the lattice constant is equal to a, whereas for the honeycomb structure the lattice constant is equal to $\sqrt{3}a$. Parameters r_1 and r_2 denote the radius of the inner rods and the outer radius of the shell layer, respectively. The thickness of the shell layer is then r_2-r_1. We prefer to describe the shell-layer thickness by introducing a new parameter β, defined as the ratio between r_2-r_1 and the outer radius r_2, i.e., $\beta=(r_2-r_1)/r_2$. Parameter β can range between 0 and 1. Note that $\beta=0$ yields rods without shell layer, while $\beta=1$ yields rods made of the shell material only, i.e., there are no inner rods.

The photonic bands of 2D photonic crystals were calculated using the finite difference time domain (FDTD) method, also known as the order (N) method.[18] In a 2D photonic crystal, the electromagnetic wave is decoupled into two polarization modes according to whether the electric field (TM modes) or the magnetic field (TE modes) is parallel to the rods. The bands for both polarization modes were independently calculated along the Γ-X-J-Γ edges of the irreducible Brillouin zone. The computational domain for the FDTD calculations consisted of one lattice unit cell, repeated infinitely by applying Bloch periodic boundary conditions. The lattice unit cell was divided up into 64×64 discretization grid points. The dielectric constant at each grid point was defined by taking the average of the dielectric constant over 10×10 subgrid points, ensuring in this way better convergence.[18] The convergence and numerical stability of the calculations were tested by increasing the grid size, i.e., using a grid of up to 100×100 points (the number of subgrid points was kept the same). The deviations in the band frequencies were found to be less than 1% for the lowest ten photonic bands. As a comparison, several tests with smaller grid size, e.g., 32×32 points, did not meet the 1% accuracy condition, showing band deviations in the order of 3%. Thus the results for the gap widths reported here (with 64×64 grid size) are believed to be accurate to within at least 1% of their true values.

III. RESULTS AND DISCUSSION

A. Triangular lattice

We begin our discussion with the triangular structure consisting of air holes drilled in silicon [Fig. 1(a)]. First, we consider the case when $\beta=0$, i.e., there is no interfacial layer. The triangular structure of circular air rods is known to have the greatest absolute PBG among the studied 2D photonic crystals.[19] Figure 2(a) shows the photonic band structure for the optimum rod radius $r_1=0.48a$, for which the absolute PBG reaches its maximum normalized width of $\Delta\omega/\omega_g=17.7\%$. Here, the normalized gap width is expressed as the ratio in percent between the frequency width $\Delta\omega$ of the gap and the frequency ω_g at the middle of the gap. The absolute PBG is formed from the overlap between the TE1-2 (i.e., the gap between the first and second photonic bands) and the TM2-3 polarization gaps. Now let us consider that a shell layer exists between the air rods and the background dielectric, i.e., $\beta>0$. Figure 2(b) shows the dispersion curves for $r_1=0.432a$ and $\beta=0.1$ considering that the shell layer is made of SiO_2 ($\varepsilon_s=3.9$). For these geometrical parameters the outer radius r_2 of the rods covered with a shell layer is exactly $r_2=0.48a$ and it is equal to the optimum rod radius for the shell-less case. We should expect that the bands decay in frequency because of the reduced air filling fraction. Indeed, the photonic bands tend to bunch towards lower frequencies. This effect is more pronounced for the higher bands, which finally leads to a decrease in the absolute PBG width. The

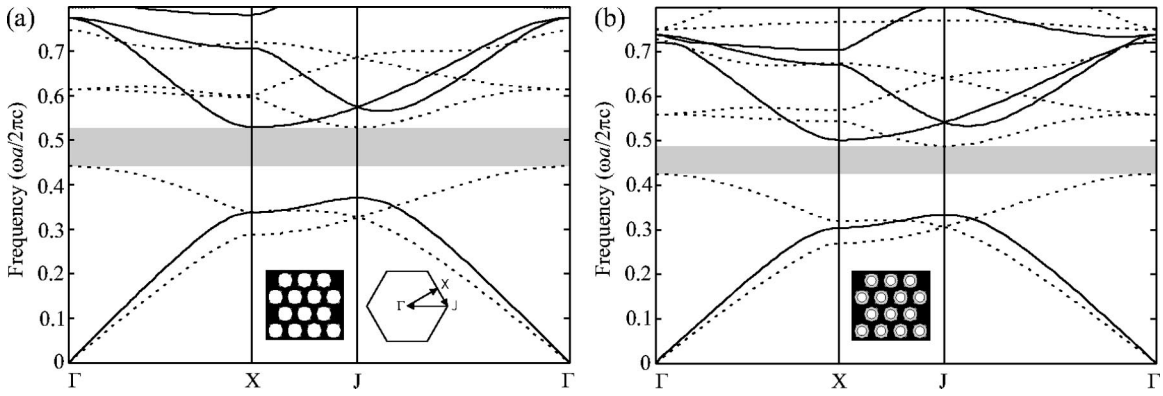

FIG. 2. Photonic bands for (a) triangular structure of air holes in silicon at $r_1=0.48a$ and (b) triangular structure of air holes in silicon with an interstitial layer of SiO_2 ($\varepsilon_s=3.9$) at $r_1=0.432a$ and $\beta=0.1$. The solid and dashed lines denote TE and TM polarization modes, respectively. The picture insets depict the structures under consideration and the irreducible Brillouin zone for the calculations. The absolute PBG is indicated by shaded area.

absolute PBG width in this case is $\Delta\omega/\omega_g=13.7\%$.

The photonic gap map in the case of rods covered with SiO_2 shell layer of thickness $\beta=0.1$ is shown in Fig. 3, where the dimensionless frequencies are plotted against the rod radius r_1/a. If we compare this map with the well-known gap map for the ideal triangular structure [for example, see Fig. 4 (Appendix C) from Ref. 1] we can see that the gaps lie at lower frequencies. The shift of gap positions towards lower values of the inner rod radius r_1 accounts for the given definition of β. The outer radius r_2 of the rods with shell layer can be calculated from $r_2=r_1/(1-\beta)$. It can be seen that the TE1-2 polarization gap is not closed for rod radii above the close-packed condition. Here, the close-packed condition is defined as the value of outer radius r_2 for which the rods covered with a shell layer begin to touch. This is always $r_2=0.5a$. The value of the inner rod radius r_1 (air rod radius) for which close packing occurs will then depend on the shell layer thickness β. For example, for $\beta=0.1$ the rods begin to touch when $r_1=0.45a$. The TE1-2 polarization gap is still opened for $r_1>0.45a$ because the triangular lattice remains

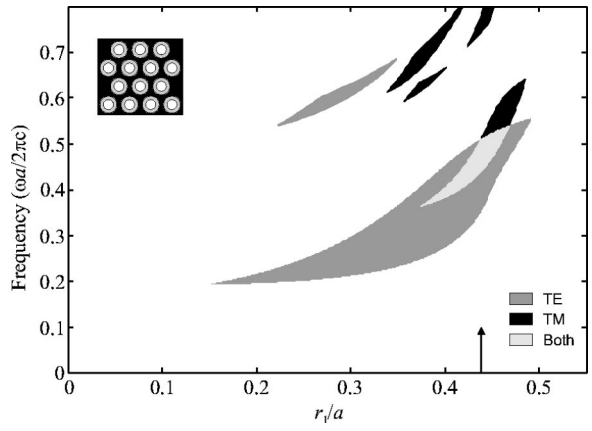

FIG. 3. Photonic gap map (normalized frequency $\omega a/2\pi c$ versus relative radius r_1/a) for the triangular structure of air rods with a SiO_2 shell layer of thickness $\beta=0.1$. The absolute PBG has a maximum width of $\Delta\omega/\omega_g=15.2\%$ for $r_1=0.438a$ (indicated by arrow).

connected through the overlapping shell layers of the neighbor rods. The TM2-3 polarization gap has a smaller width than for the ideal case leading to narrower absolute photonic gap. The largest gap-midgap ratio for this structure is $\Delta\omega/\omega_g=15.2\%$ reached for $r_1=0.438a$.

Note that for $r_1=0.438a$ and $\beta=0.1$, the thickness of the shell layer is approximately $0.049a$, so the outer diameter r_2 of the air rods, "covered" with SiO_2 is $r_2=0.487a$. It seems that the maximum absolute PBG occurs for almost the same rod diameter as when there is no shell layer. This is because for lower values of β and for shell layers of low dielectric constant, for instance SiO_2, the effective dielectric constant remains almost unchanged. However, for higher values of β and for shell layers of high dielectric constant, the effects of the interfacial layer on the absolute PBG cannot be trivially deduced. The dependence of the absolute PBG on the thickness β and the dielectric material ε_s of the shell layer can be traced from the next two figures. In Fig. 4 the normalized width of the absolute PBG is plotted against the radius r_1 of the air rods for several values of the parameter β and for the three shell materials considered here. The case without shell layer ($\beta=0$) is also shown for the purposes of comparison. For the case of SiO_2 shell layer, it can be seen that as the thickness of the layer increases, the position of maximum absolute PBG shifts towards lower values of the rod radius r_1. The absolute PBG reaches its maximum for values of r_1 below the close-packed condition (indicated by a short vertical bar). Unlike the inner rod radius r_1, the value of outer rod radius r_2 which gives the largest absolute PBG remains close to $0.48a$, as for the shell-less case. Figure 5 shows the dependence of the maximum gap width on the shell layer thickness β. For the case of SiO_2 layer, the maximum width of the absolute PBG decreases for values of $\beta>0$, and for $\beta>0.33$ the absolute gap completely disappears. For greater values of β, the air rods have a thick SiO_2 cladding, so the structure resembles now a triangular structure formed mostly of SiO_2 rods embedded in silicon. This structure does not exhibit an absolute PBG because of the low dielectric contrast $\varepsilon_b/\varepsilon_s$.

The overall behavior of the absolute PBG in the case of Si_3N_4 shell layer ($\varepsilon_s=7.5$) is similar to the previous case.

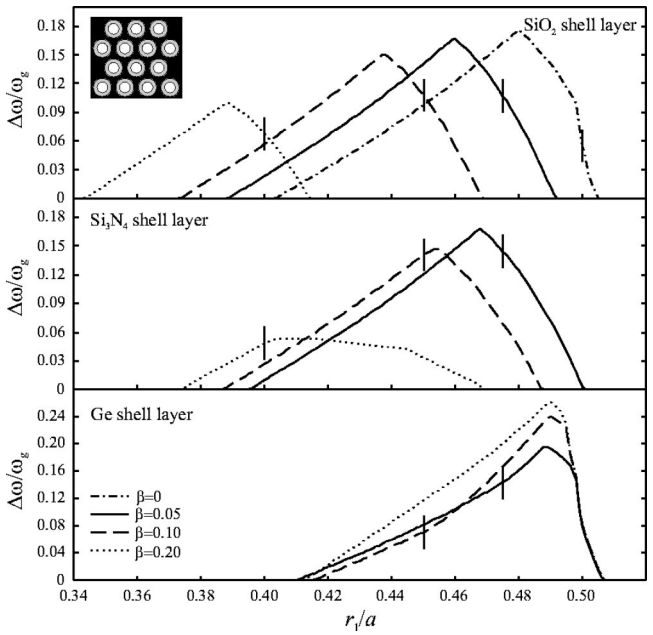

FIG. 4. Width $\Delta\omega/\omega_g$ of the absolute PBG as a function of the rod radius r_1 for the triangular structures of air rods covered with SiO_2, Si_3N_4, or Ge shell layers of different thicknesses β. The vertical bar marker indicates the close-packed condition, which is $r_{1cp}=0.5$, 0.475, 0.45, and 0.4 for $\beta=0$, 0.05, 0.1, and 0.2, respectively.

The existence of a shell layer always leads to a smaller absolute gap (Fig. 5). However, the absolute PBG width decreases more rapidly and, for values of $\beta>0.25$, it is almost zero. The position of the maximum absolute PBG is no longer as predictable as it was for the SiO_2 shell layer. For example, in the case of the SiO_2 shell layer, it was found that the absolute PBG reached its maximum width for outer radius r_2 near $0.48a$, regardless of the shell layer thickness β. In the case of Si_3N_4, however, the absolute PBG does not follow the same rule. For $\beta=0.1$, the absolute PBG has a maximum when $r_1=0.454a$, so the outer radius should be $r_2=0.504a$. The outer radius r_2 becomes greater than the close-packed condition and the shell layers of adjacent rods should therefore overlap. The critical value of the shell layer thickness β, for which the maximum absolute PBG width appears at the close-packed condition, is $\beta=0.09$. For $\beta>0.09$, the absolute PBG decreases sharply because the optimum outer radius r_2 already approaches the filling-space condition. The filling-space condition is defined as the radius for which the rods entirely fill the area of the unit cell. For the triangular structure, this is $r_2=0.577a$. For shell layer thickness greater than 0.09, the optimum gap is reached when the rods actually overlap. Therefore the photonic structure consisting of Si_3N_4-clad air rods embedded in silicon background becomes a structure comprising air rods embedded in Si_3N_4 background, instead of silicon. Because of the low dielectric contrast, the triangular lattice of air rods in Si_3N_4 presents a very small absolute PBG width of about $\Delta\omega/\omega_g=2.8\%$.

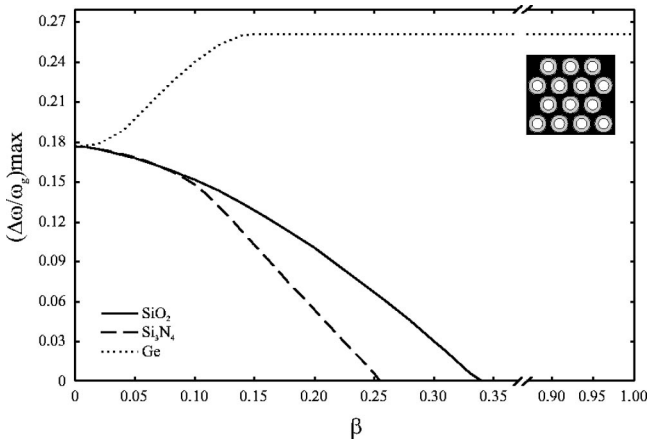

FIG. 5. Maximum width of the absolute PBG as a function of the shell-layer thickness β for the triangular lattice of air rods "covered" with SiO_2 ($\varepsilon_s=3.9$), Si_3N_4 ($\varepsilon_s=7.5$), or Ge ($\varepsilon_s=16$) shell layer.

The behavior of the absolute PBG drastically changes when the air rods are covered with Ge($\varepsilon_s=16$) shell layer. The dielectric constant of the shell layer is now greater than that of background material. It should be expected that the existence of an interstitial layer would improve the absolute PBG because of higher dielectric contrast ($\varepsilon_s/\varepsilon_r$) at the air rod interface. Indeed, the absolute PBG has greater magnitudes than in the shell-less case ($\beta=0$) (Fig. 5). The gap width increases as the shell layer gets thicker. For example, for $\beta=0.2$ the maximum absolute PBG width is $\Delta\omega/\omega_g=26.2\%$ at $r_1=0.49a$. However, the optimum absolute PBG always happens to occur above the close-packed condition. Moreover, when $\beta>0.15$ it occurs for rod radii above the filling-space condition, so the structure we actually investigate is a triangular structure of air rods embedded in Ge background matrix. For radius r_1 far from the close-packed condition, the absolute PBG width is always less than in the shell-less case.

Having discussed the triangular structure of air rods covered with a shell layer and embedded in silicon, we shall now study the inverse arrangement, i.e., silicon rods covered with a shell layer and embedded in air. For the shell-less silicon rods ($\beta=0$), it is well known that the triangular structure does not exhibit any absolute PBG because of disrupted lattice connectivity. Neither does the existence of a shell layer ($\beta>0$) contribute to the opening of an absolute PBG. We can use the heuristic in Ref. 1 , which holds that the connectivity of high- ε regions is conducive to TE gaps, and that isolated islands of high-ε material lead to TM gaps. Then there is no reason for the absolute PBG opening because the shell layer does not form any connected structure. We think it would be interesting to see how the shell layer affects the properties of the first TM polarization gap (TM1-2), which is about $\Delta\omega/\omega_g=48.9\%$ for the shell-less triangular structure. Figure 6 shows how the maximum width of the TM1-2 gap depends on the shell layer thickness β for the three dielectric materials considered. We can see that if the dielectric constant of the shell material is less than that of silicon, the gap diminishes when the thickness of the shell layer increases. For germanium, whose dielectric constant is greater than that of silicon, the reverse is true: the gap widens as β increases. For $\beta=1$, the silicon rods covered with a shell

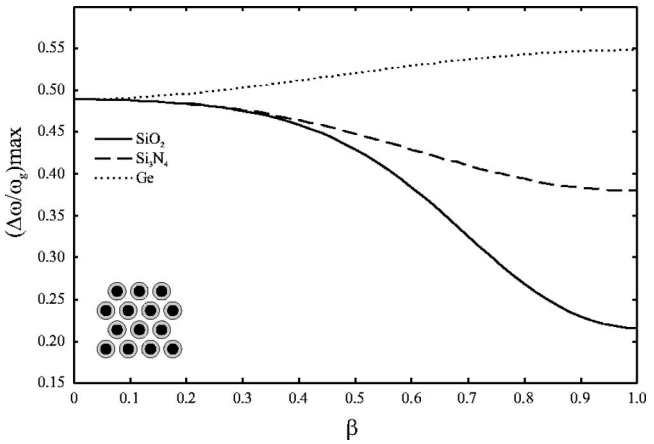

FIG. 6. Maximum width of the TM1-2 polarization gap as a function of the shell layer thickness β for triangular structure of silicon rods in air.

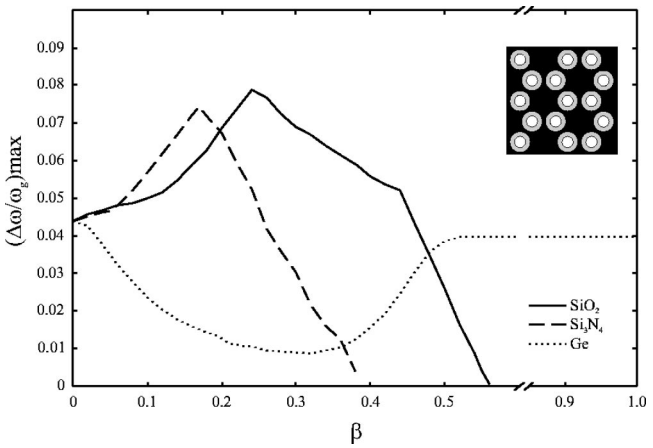

FIG. 7. Optimal width of the absolute PBG as a function of the shell layer thickness β for the honeycomb lattice of air rods embedded in silicon.

layer are transformed into rods made of the corresponding shell material. Therefore for the triangular structure of dielectric rods with a shell layer, the width of the TM1-2 polarization gap always ranges between its values for $\beta=0$ (shell-less rods) and $\beta=1$ (rods entirely replaced by the shell layer).

These results suggest that the gap behavior is governed by the dielectric contrast at the shell layer–air interface. Covering the rods with materials of low dielectric constant will reduce the width of the gap, while high-dielectric claddings will improve the gap size. However, for the triangular structure of air rods in dielectric media, this improvement is fictitious because it appears for infeasible rod diameters. Any interfacial layers for this arrangement should be therefore avoided.

B. Honeycomb lattice

In this section, we focus on the honeycomb lattice consisting of rods covered with a shell layer. In the ideal case (shell-less rods), the honeycomb arrangement of air holes in dielectric media exhibits a narrow absolute PBG due to the weak overlap between TE5-6 and TM6-7 polarization gaps (see, for example, Fig. 2 of Ref. 9). In the particular case of air rods embedded in silicon background, this absolute PBG has an optimum width of $\Delta\omega/\omega_g=4.4\%$ for $r_1=0.484a$, which is very close to the close-packed condition. The evolution of this absolute PBG, when an interfacial layer is present between the air rods and the background silicon, is rather strange. Figure 7 shows its optimal width as a function of the shell layer thickness for the three shell materials considered. It can be seen that shell layers of lower dielectric constants, i.e., SiO_2 and Si_3N_4, yield an improvement in the absolute PBG size, whereas shell layers of higher dielectric constants, i.e., Ge, reduce the gap width. This gap behavior is just opposite to the already discussed one for the triangular lattice of air rods in silicon. We notice that the observed improvement in the absolute PBG size always occurs for rod radii above the close-packed condition ($r_2=0.5a$). Near the close-packed condition, the honeycomb lattice of air rods in dielectric resembles a triangular structure with lattice constant $\sqrt{3}a$ formed by dielectric rods of noncircular cross section and embedded in air.[9] Therefore for rod radii above the close-packed condition we actually examine the triangular structure comprising noncircular dielectric rods in air. The unfeasible rod diameters and the really small width of the absolute PBG make the honeycomb lattice of air rods in dielectric worthless for practical realization.

The most prominent feature of the honeycomb structure is that, in the case of dielectric rods embedded in air, it exhibits an absolute PBG, so in a sense it is complementary to the triangular structure discussed in the previous section. Also, the absolute PBG occurs at filling fractions that are far from the close-packed condition, which makes the fabrication of such 2D photonic crystals less formidable. In Fig. 8(a) we plot the dispersion relation for the shell-less honeycomb lattice at $r_1=0.247a$. An absolute photonic gap opens up from the overlap between TE5-6 and TM7-8 polarization gaps. For the given rod radius, this absolute PBG has a maximum normalized width of $\Delta\omega/\omega_g=10\%$. Let us cover now the silicon rods by SiO_2 of thickness $\beta=0.1$, so that the outer radius r_2 of the rods with a shell layer remains $r_2=0.247a$. Figure 8(b) plots the dispersion relation for this case and we can see that the bands go to higher frequencies since the effective dielectric constant is reduced. The gap width ($\Delta\omega/\omega_g=9.4\%$) is slightly decreased compared to the ideal (shell-less) structure. Figure 9 shows the photonic gap map for this modified honeycomb lattice considering that the rods are covered with SiO_2 layer of thickness $\beta=0.1$. As for the shell-less honeycomb lattice (see, for example, Fig. 4 from Ref. 9), three absolute photonic gaps are present, which appear and have their maxima for different rod dimensions. The highest absolute PBG is formed from the overlapping TE5-6 and TM7-8 polarization gaps. Hereafter, to avoid ambiguity and repetition, we will refer to this absolute PBG as the G1 gap. The lowest one is due to the overlap between TE3-4 and TM6-7 gaps. It will be referred to as the G2 gap. Finally, the overlapping TE5-6 and TM6-7 polarization gaps give rise to a small absolute PBG, which will be referred to as the G3 gap. In addition to these three absolute PBG a weak overlap

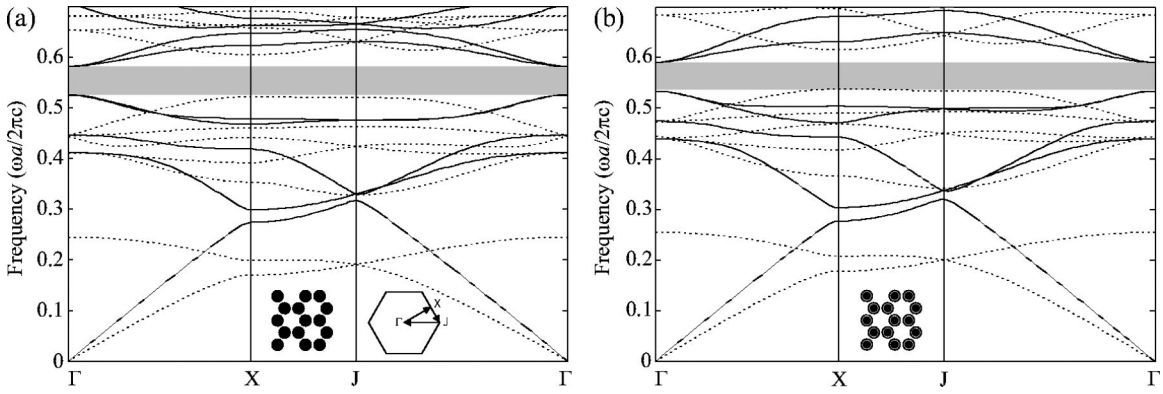

FIG. 8. Photonic band structures for the honeycomb lattice of silicon rods in air: (a) shell-less rods with radius $r_1=0.247a$ and (b) rods with inner radius $r_1=0.222a$ (outer radius $r_2=0.247a$) covered by SiO_2 with thickness $\beta=0.1$. The solid and dashed lines represent the TE and TM modes, respectively. The frequency range of the absolute PBG is indicated by a shaded patch.

can be seen between the TE1-2 and TM2-3 polarization gaps (Fig. 9), which is not observed in the gap map of the ideal honeycomb structure. However, the gap size of this new absolute PBG is too small to be used, so we do not concern ourselves with this band-gap region. The largest absolute photonic gap for the present case is the G1 gap, which reaches its maximum width of $\Delta\omega/\omega_g=9.6\%$ for $r_1=0.234a$. Therefore it seems that the existence of an interfacial layer surrounding the silicon rods reduces the size of the largest absolute PBG for the studied structure. But, we will show that the interfacial layer could favor the other absolute PBG's, increasing their initially smaller magnitudes, and could even give rise to larger gaps compared to the shell-less structure. We have studied how the three substantial absolute PBG's (G1, G2, and G3) for the structure shown in Fig. 1(b) evolve with respect to the material and thickness of the shell layer covering the silicon rods.

Figure 10 shows the normalized widths of these absolute PBG's as functions of the rod radius r_1 for three different thicknesses of the shell layer made of SiO_2. Again, the case without shell layer ($\beta=0$) is also shown for purposes of comparison. The G1 gap decreases slightly with increasing the shell layer thickness β, whereas the other two gaps G2 and G3 are more strongly affected. This is particularly due to the variations in the filling fraction for different radii r_1. From the definition of parameter β, according to whether the inner rod radius r_1 is small or high, the shell layer will be thinner or thicker for fixed value of β. Since the G2 and G3 gaps arise for higher values of r_1, the introduced amount of the shell material is greater than in case of smaller r_1, so these gaps appear to be more sensitive to changes in β. Nevertheless, the overall tendency for the G1 and G2 gaps is the same. These gaps shrink when a shell layer is present, whereas the G3 gap widens. It should be noted that in the present case the close-packed condition ($r_2=0.5a$) is never reached.

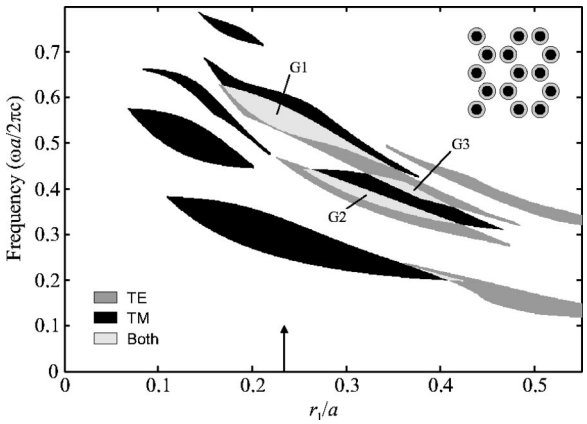

FIG. 9. Photonic gap map for the honeycomb lattice of silicon rods in air covered with SiO_2 layer of thickness $\beta=0.1$. Three absolute PBG's are observed, denoted as G1, G2, and G3 absolute gaps. The arrow indicates the position $r_1=0.234a$ of the largest absolute PBG with a maximum width of $\Delta\omega/\omega_g=9.6\%$.

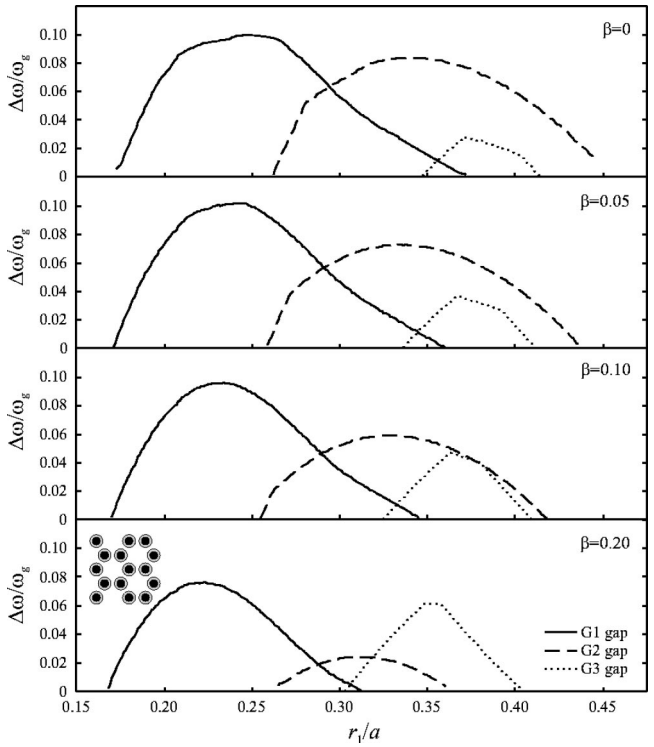

FIG. 10. Normalized widths of the three absolute PBG's (G1, G2, and G3) for the honeycomb lattice plotted against the inner rod radius r_1 for three shell layer thicknesses $\beta=0.05$, 0.10, and 0.20. The considered shell layer material is SiO_2 ($\varepsilon_s=3.9$). The shell-less case ($\beta=0$) is also shown.

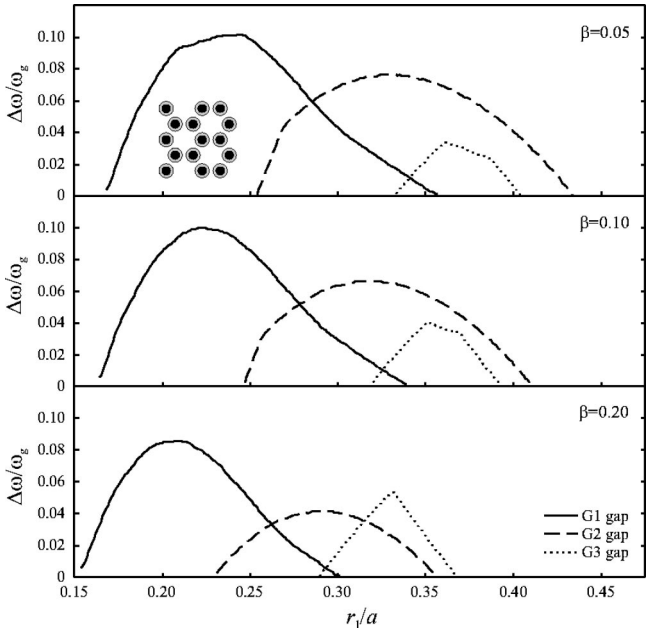

FIG. 11. Normalized widths of the three absolute PBG's (G1, G2, and G3) for the honeycomb lattice plotted against the rod radius r_1 for three shell layer thicknesses β. The shell layer material studied is Si_3N_4 ($\varepsilon_s=7.5$).

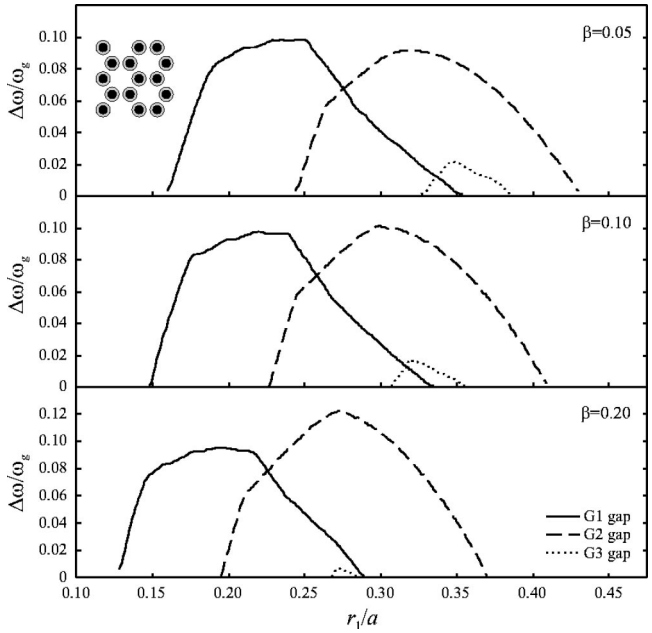

FIG. 12. Normalized widths of the G1, G2, and G3 absolute gaps for the honeycomb lattice plotted against the rod radius r_1 for three shell layer thicknesses β. The shell layer material studied is Ge ($\varepsilon_s=16$).

Almost the same happens in the evolution of the gaps when a shell layer of Si_3N_4 is considered (Fig. 11). We will discuss here only the main differences in gap behavior with respect to the previous case. The G1 and G2 absolute gaps are much less affected by the thickness of the shell layer and decrease slightly as β increases. The increase in the G3 gap, however, is lower than in the case of SiO_2 shell layer. The maximum width reached for $\beta=0.2$ is $\Delta\omega/\omega_g=5.3\%$, compared to $\Delta\omega/\omega_g=6.1\%$ in the case of SiO_2.

If the shell layer is made of Ge, whose dielectric constant is greater than that of silicon rods, the absolute PBG's evolve in a completely different way (Fig. 12). For example, the G3 gap is disappointingly small and for values of $\beta>0.24$ it becomes fully suppressed. Fortunately, the G1 gap, which was the largest one for the shell-less honeycomb lattice, is not altered at all by the thickness of the shell layer. Even at $\beta=0.2$, its width $\Delta\omega/\omega_g=9.6\%$ remains almost the same as for the shell-less case. Moreover, the G2 gap now shows a relative width $\Delta\omega/\omega_g=12.2\%$ and so becomes the largest gap for the structure. It lies at lower frequencies and so it becomes more robust to imperfections generated by the fabrication. When β increases, the width of the G2 gap approaches its value for the case of honeycomb lattice comprising germanium rods rather than silicon rods in air. Our structure consisting of silicon rods with Ge coating is therefore mainly seen as a structure formed of germanium rods, even for thin interfacial layers. This claim is justified in the Fig. 13, which plots the optimum widths of the absolute gaps against the shell layer thickness. The lower ($\beta=0$) and upper ($\beta=1$) limits of the parameter β represent the two special cases, i.e., shell-less structure and structure where the rods are made of the shell material, respectively. When SiO_2 and Si_3N_4 layers are considered, the width of the G1 gap decreases, but for the Si_3N_4 layer the gap width does not fall below 2.4% at $\beta=1$. Indeed, this is the width of the G1 gap for the honeycomb lattice of Si_3N_4 rods embedded in air. Because of the low dielectric contrast, this lattice does not exhibit any other absolute PBG's. The honeycomb structure consisting of SiO_2 rods in air has no absolute PBG's for the same reason. In the case of Ge rods in air, the width of the G1 gap is about 9%, so the G1 gap for silicon rods with Ge

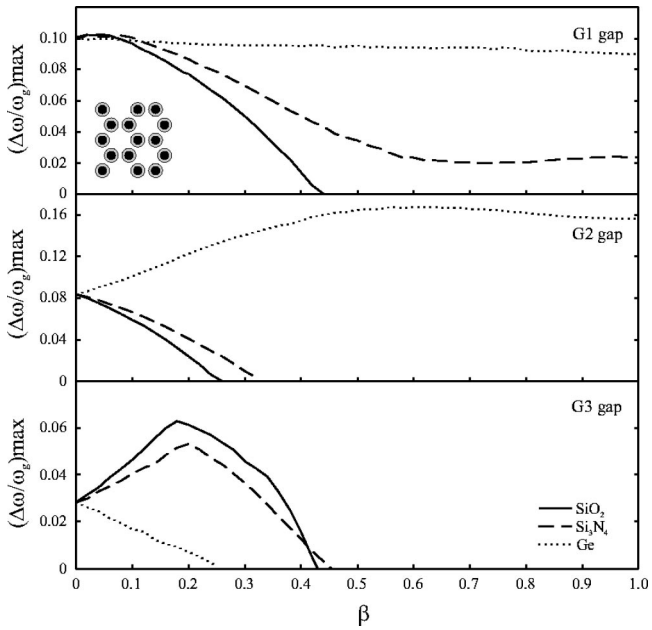

FIG. 13. Optimal widths of the G1, G2, and G3 absolute photonic gaps as functions of shell layer thickness β for the three dielectric materials considered SiO_2, Si_3N_4, and Ge. The lower $\beta=0$ and upper $\beta=1$ limits represent the shell-less honeycomb lattice with rods made of silicon or of the shell dielectric, respectively.

cladding stands near this value as β increases. The G2 gap behaves in a similar way, i.e., it increases towards the value $\Delta\omega/\omega_g = 15.6\%$, which is the gap width for the special case of Ge rods embedded in air.

To conclude, it should be pointed out that the honeycomb arrangement of dielectric rods is suitable for the fabrication of PBG materials because the largest absolute gaps are attainable for reasonable rod diameters, which avoids the tricky achievement of thin dielectric voids. In addition, our results provide further flexibility in the realization of these materials. For example, in certain cases we may not be able to obtain pillars (rods) of the required diameter or of the particular material we need, because of technological limitations. However, we are enabled to grow the rods of materials with lower dielectric constants, for which a well-developed technology exists. The rods can then be covered with the required dielectric by some depositing technique, thus achieving almost the same gap properties as those of the ideal shell-less structure.

IV. CONCLUSIONS

We have performed a detailed quantitative analysis of the absolute PBG's in 2D triangular and honeycomb lattices considering that an interfacial layer is present between the rods and the background matrix. Both complementary structures, i.e., air rods in a dielectric and dielectric rods in air have been studied. The properties of the photonic gaps are strongly affected by the thickness and the dielectric constant of this interfacial layer. The following general conclusions about the absolute PBG evolution can be drawn:

(i) For structures consisting of air rods in a dielectric background, the existence of an interfacial layer always entails a reduction in the absolute PBG width and should therefore be avoided. The decrease in the gap width depends mainly on whether the dielectric constant of the interfacial layer is greater or less than that of the background matrix. Higher dielectric constant of the shell layer entails gaps which are practically unattainable. If for any reasons an interfacial layer is desired, small thicknesses and low dielectric constants should be chosen because the gap properties will be only slightly affected.

(ii) For structures formed of dielectric rods in air, interfacial layers with lower dielectric constants yield gaps with smaller widths than in the shell-less case. The rate of decrease is as high as the dielectric constant of the shell material is low. However, shell layers whose dielectric constants are higher than that of the rod material lead to larger absolute photonic gaps. The gap size is increased up to values that are typical for the structure consisting of rods made only of the shell dielectric.

The interfacial layer can be treated as hollow ring-shaped rods included at the center of each basic rod of the lattice unit cell. However, we notice that the concept of including an interfacial layer into the basic unit cell does not deal at all with the symmetry reduction approach because this inclusion does not modify the symmetry properties of the lattice or those of the scatterers. The gap behavior is ruled by the dielectric constant and the filling fraction of the included material and reflects the induced changes in the effective dielectric constant of the crystal. Although we have considered here a few 2D lattices, nevertheless, the given approach is not essential and can be applied to other 2D as well 3D photonic structures.

ACKNOWLEDGMENTS

This work was supported by the Spanish Commission of Science and Technology (CICYT) under Grant No. TIC2002-04184-C02. We thank the Supercomputing Center of Catalonia (CESCA) for an allowance of computer time.

*Author to whom correspondence should be addressed. Electronic address: lmarsal@etse.urv.es

[1] J. D. Joannopoulos, R. D. Meade, and J. N. Winn, in *Photonic Crystals, Molding the Flow of Light* (Princeton University Press, Princeton, NJ, 1995).
[2] S. John, Phys. Rev. Lett. **58**, 2486 (1987).
[3] E. Yablonovitch, Phys. Rev. Lett. **58**, 2059 (1987).
[4] D. L. Bullock, C.-C. Shih, and R. S. Marguiles, J. Opt. Soc. Am. B **10**, 399 (1993).
[5] J. C. Knight, J. Broeng, T. A. Birks, and P. S. J. Russell, Science **282**, 1476 (1998).
[6] R. F. Cregan, B. J. Mangan, J. C. Knight, T. A. Birks, P. S. J. Russell, P. J. Roberts, and D. C. Allan, Science **285**, 1537 (1999).
[7] M. Plihal andA. A. Maradudin, Phys. Rev. B **44**, 8565 (1991).
[8] P. R. Villeneuve and M. Piché, Phys. Rev. B **46**, 4973 (1992).
[9] D. Cassagne, C. Jouanin, and D. Bertho, Phys. Rev. B **52**, R2217 (1995).
[10] M. Qiu and S. He, Phys. Rev. B **60**, 10 610 (1999).
[11] L. F. Marsal, T. Trifonov, A. Rodríguez, J. Pallarès, and R. Alcubilla, Physica E (Amsterdam) **16**, 580 (2003).
[12] T. Trifonov, L. F. Marsal, A. Rodríguez, J. Pallarès, and R. Alcubilla,Phys. Rev. B **69**, 235112 (2004).
[13] J. Schilling, R. B. Wehrspohn, A. Birner, F. Müller, R. Hillebrand, U. Gösele, S. W. Leonard, J. P. Mondia, F. Genereux, H. M. van Driel, P. Kramper, V. Sandoghdar, and K. Busch, J. Opt. A, Pure Appl. Opt. **3**, S121 (2001).
[14] V. Lehmann, J. Electrochem. Soc. **140**, 2836 (1993).
[15] T. Pan and Z.-Y. Li, Solid State Commun. **128**, 187 (2003).
[16] T. Baba and T. Matsuzaki, Jpn. J. Appl. Phys., Part 1 **35**, 1348 (1996).
[17] S. M. Sze, in *Physics of Semiconductor Devices* (Wiley-Interscience, New York, 1981).
[18] C. T. Chan, Q. L. Yu, and K. M. Ho, Phys. Rev. B **51**, 16 635 (1995).
[19] R. D. Meade, K. D. Brommer, A. M. Rappe, and J. D. Joannopoulos, Appl. Phys. Lett. **61**, 495 (1992).